

PPS021-01

Room:101

Time:May 23 08:30-08:45

Development of Laser Ionization Mass Nanoscope: LIMAS

Shingo Ebata^{1*}, Morio Ishihara¹, Kiichiro Uchino², Satoru Itose³, Miyuki Matsuya³, Masato Kudo³, Hisayoshi Yurimoto⁴

¹Osaka University, ²Kyushu University, ³JEOL Ltd., ⁴Hokkaido University

Many sample-return missions are planned in the world (e.g. JAXA Hayabusa, NASA Stardust). Samples are collected on asteroids or comets, returned to the Earth, and then analyzed in laboratories. However, a very small amount of samples can be brought back because of the limitations on the space probes. Thus ultra-high sensitivity, lateral resolution, and resolving power are required for the mass spectrometer.

Here we have been developing a novel TOF-SIMS system; prototype in Osaka Univ. and new-type in JEOL Ltd.. This instrument consists of a FIB system with a liquid metal Ga ion source, a femto-second laser for post-ionization and a multi-turn TOF-MS 'MULTUM II'.

Firstly, in order to evaluate the performance of quantitative analysis, several alloys and standard glass JB-2 were analyzed using the prototype system. Alloys used for this evaluation were Constantan, Cupronickel, Brass, Inconel-625, SUS301, SUS310, and SUS321 (the Nilako corp., Japan).

Secondly, in order to evaluate the postionization efficiency and mass resolving power using the new-type system 'LIMAS', non-postionization (SIMS) and postionization mode were compared. Samples used for this evaluation were Al for SIMS mode and Ag substrate for postionization mode, respectively.

Chemical compositions of constantan, cupronickel, and brass were corresponded approximately to reference values in the error ranges. Chemical compositions of SUS301, SUS310 and SUS321 were slightly higher intensity of Cr and slightly lower of Ni than those of reference values. These results show this instrument was useful for quantitative analyses. On the other hand, Chemical compositions of inconel-625 was very higher of Cr than those of reference value.

The postionization efficiency and mass resolution using the new-type system 'LIMAS' were evaluated. By using post-ionization, the secondary ion signals of Ag were increased ~6000 times compared with the conventional TOF-SIMS experiments. This result shows that the nonresonant multiphoton post-ionization experiments have superior sensitivity. Compared to the prototype experiments, the secondary ion signals of Ag were increased ~3 times, because the pulse width of a femto-second laser was improved from 120 fs to 40 fs.

The mass resolution was achieved to ~12000 by SIMS mode (flight length: ~70 m at 50 cycles) and ~15000 by LIMAS mode (flight length: ~35 m at 25 cycles). These results show this instrument was useful for isotope analyses.

These results indicated that this instrument would be very effective for ultrahigh sensitivity analysis of nano-size particles such as Hayabusa mission return samples.

Keywords: Hayabusa, SNMS, Focused ion beam, Femto second laser, Multi-turn mass spectrometry

PPS021-02

Room:101

Time:May 23 08:45-09:00

Microspectroscopic analysis of iron meteorite using photoelectron emission microscopy (PEEM)

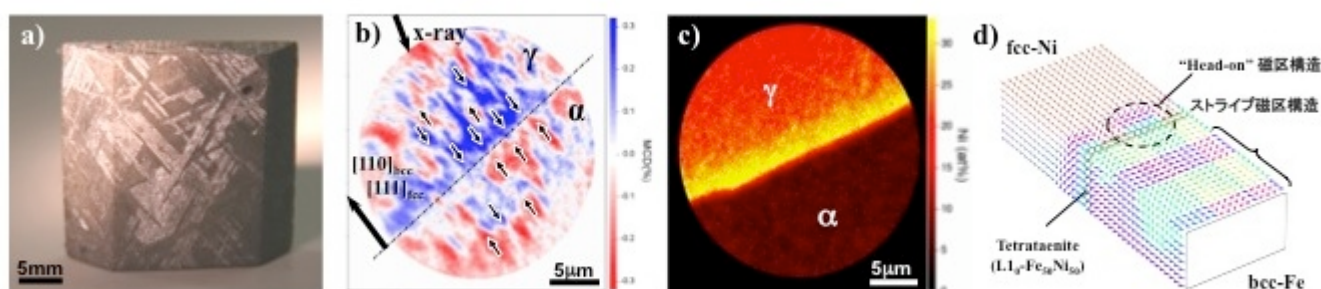
Masato Kotsugi^{1*}

¹SPring-8/JASRI

The magnetic properties of iron meteorites greatly differ from those of iron-nickel alloys found on Earth, the reason for which has long been veiled in mystery. The scientists of this research team approached this mystery of the magnetic properties of iron meteorites by accurately evaluating their physical properties from the viewpoint of materials science and, at the same time, considering that such accurate evaluation will be effective for the exploration of other magnetic materials.

They directly observed iron meteorites at the nanometer level using a photoemission electron microscope (PEEM) at SPring-8, and discovered a new magnetic domain structure, which has never been found in conventional iron-nickel alloys. (PEEM is a cutting-edge microscope that came under the spotlight because of its use in the research awarded the 2007 Nobel Prize in Chemistry.) By comparing the magnetic domain structure obtained in the experiments with that obtained by simulation, it was clarified that the magnetic domain structure originates from tetrataenite, an iron-nickel phase unique to iron meteorites.

This tetrataenite phase, originating from the universe, does not contain rare metals and exhibits excellent functionalities; therefore, it is expected to lead to the achievement of high density and power saving as well as resource saving in next-generation magnetic devices. Currently, the artificial creation of tetrataenite and the evaluation of its physical properties are ongoing, aiming towards its application to such devices, which are expected to have a productive ripple effect on future green nanotechnology.



Keywords: iron meteorite, synchrotron radiation, photoelectron emission microscopy, microscopy, magnetic structure, paleomagnetism

PPS021-03

Room:101

Time:May 23 09:00-09:15

Nondestructive characterization of a single micron-sized primitive-grain realized by magnetic ejection in microgravity

Keiji Hisayoshi^{1*}, Chiaki Uyeda¹

¹Graduate School of Science, Osaka Unives

A new principle is proposed for the characterization of a single grain sample. This principle is based on a translation induced by a magnetic field-gradient force that was recently found on diamagnetic solids [1][2]. A single mm-sized sample was released in an area field gradient that was located in microgravity condition. According to a motional equation of translation, acceleration of sample was uniquely determined by intrinsic magnetic susceptibility of the material in a given field distribution. Hence susceptibility of the sample was detected by observing field-induced motion of the sample. Since a published value of diamagnetic susceptibility exist for a solid material, the identification of material is possible by comparing the measured susceptibility data with the compiled list of published values. Conventional magnetization measurements in normal gravity are generally prevented by background signal of sample holder when size of sample is smaller than 1 mm in diameter. The mass measurement of the sample is difficult below the level of 100 micro grams . In contrast, it is expected that the proposed method can measure susceptibility of a single grain with limitlessly small size, provided that the observation of the grain motion is possible; material identification of the small becomes possible as well.

The conventional facilities of microgravity are not suitable for a routine analysis such as the present measurement of susceptibility. This is because the facility system requires a long machine time; its running cost is considerably high. Therefore, a compact microgravity system, which can be introduced in an ordinary laboratory, was newly developed. The length of the drop shaft is 1.5m, and the duration of microgravity time is 0.62 second. The experimental apparatus was set inside a rectangle box which had a size of 30cmx30cmx20cm. The vacuum chamber equipped with an electric actuator, sample releasing signal reception device, the sample holder controller, the magnet, the battery, and the high-vision video camera are installed in the box. The sample is released in the field-gradient produced by a by a magnetic circuit composed by a NdFeB permanent magnet. Maximum field intensity of the circuit was 0.7 T. The box was attached to the sealing of the laboratory room by an electromagnetic lock system. The free fall of the box started shortly after the power supply of the lock was shut down. Image of sample translation was recorded by the HV camera.

In the present work, translation was observed for small particle as small as 50 micron for graphite and the diamond. The spatial and time resolution of the present system can be improved by introducing a macro-lens, and by recording the image by a high-speed photography. The above mentioned improvements is expected to identify the sample of about 20 micron. If a single small particle can be identified nondestructively, the possibility of analyzing individual particle that compose primitive meteorite is expected to increase drastically. The observed magnetic susceptibility is in the range of -5×10^{-6} emu/g from -2×10^{-7} . It is expected that the diamagnetic susceptibility of the organic matter contained in the meteorites distribute in this range.

[1] K. Hisayoshi, S. Kanou and C. Uyeda: J.Phys.:Conf.Ser., 156 (2009) 012021

[2] C. Uyeda, K. Hisayoshi and S. Kanou: Jpn. Phys. Soc. Jpn. 79 (2010) 064709

Keywords: diamagnetic susceptibility measurement, nondestructive characterization, microgravity, magnetic ejection, field gradient force

PPS021-04

Room:101

Time:May 23 09:15-09:30

Oxygen isotopic compositions of melilite in Fluffy Type A CAI from Efremovka meteorite

Noriyuki Kawasaki^{1*}, Naoya Sakamoto², Hisayoshi Yurimoto³

¹Natural History Sci., Hokudai, ²CRIS, Hokudai, ³Natural History Sci., Hokudai

Calcium-Aluminum-rich inclusion (CAI) is the oldest rock in the solar system and preserves a record of events in the early solar system. Reversely zoned crystals of melilite have been found in Fluffy Type A CAIs, and have been condensed directly as solids from a hot nebular gas in the early solar system (MacPherson and Grossman 1984). In this study, oxygen isotopic compositions and chemical compositions of melilite crystals in a Fluffy Type A CAI of Efremovka CV3 chondrite has been described. A polished thin section of the CAI was used. Petrographic studies and the chemical compositions have been measured by a field emission type secondary electron microscope equipped with an energy dispersive spectrometer (FE-SEM-EDS, JEOL JSM-7000F; Oxford INCA Energy). Crystal orientations of the CAI melilite have been determined by an electron back scattered diffraction system (EBSD, HKL Channel 5) equipped with the SEM in order to determine crystal boundaries of the melilite grains. Oxygen isotopic compositions have been measured by secondary mass spectrometry (SIMS, Cameca ims-1270).

The CAI is 10 x 3 mm in size with fluffy shape. The CAI has core-mantle structure. The core part contains of large amounts of spinel which are poikilitically enclosed by anorthite, melilite and Al-Ti-rich diopside. The mantle part mainly consists of melilite, Al-Ti-rich diopside. The abundance of spinel is smaller than in the core part. A Wark-Lovering Rim (WL-Rim) surrounds the mantle. Typical size of mantle melilite crystal is 15-25 micrometers. From the distribution of chemical compositions and oxygen isotopic compositions of melilite in the mantle are classified into two distinct regions.

The first region in the mantle, domein-1, shows that melilite crystals positioned shallower than ~200 micrometers in depth from the WL-Rim have grown as reverse zoning. Compositions of the crystal center and grain boundary are $\delta^{18}\text{O} \sim 25$ and $\delta^{18}\text{O} \sim 5$, respectively. The oxygen isotopic compositions of single crystals are distributed homogeneously within the analytical error. However, oxygen isotopic compositions are systematically changed among crystals. The melilite crystals positioned near WL-rim are more ^{16}O -rich ($\text{DELTA-17O} = -19$ permil) while the melilite crystals near the CAI core are ^{16}O -poor ($\text{DELTA-17O} = -4$ permil). The oxygen isotopic compositions change continuously from rim to core of the CAI.

The second region in the mantle, domein-2, melilite crystals positioned shallower than ~40 micrometers in depth from the WL-Rim have grown as reverse zoning. Compositions of the crystal are $\delta^{18}\text{O} \sim 25$ in the center and $\delta^{18}\text{O} \sim 8$ at the grain boundary. While the melilite crystals of domein-2 positioned deeper than the ~40 micrometers have grown initially as reverse zoning and then grown as normal zoning, i. e., oscillated. The compositions are $\delta^{18}\text{O} \sim 30$ in the center, $\delta^{18}\text{O} \sim 45$ in the intermediate, and $\delta^{18}\text{O} \sim 55$ at the grain boundary. Typical width of the normal zoning part is 2-5 micron. Oxygen isotopic composition of melilite crystals existed in the domein-2 are homogeneously distributed, $\text{DELTA-17O} = -3$, despite of complex growth patterns.

The oxygen isotopic heterogeneity observed in the domein-1 suggests that oxygen isotopic ratios of nebular gas surrounding the melilite growing did not changed during the growth of each melilite crystal, while gradually changed from ^{16}O -poor to ^{16}O -rich during the total duration of melilite formation of domein-1. In this nebular condition, the melilite was directly condensed from the nebular gas and accumulated together. The oxygen isotopic compositions observed in domein-2 suggest that the melilite seems to be directly condensed from ^{16}O -poor nebular gas and accumulated together. Then the domein-1 and domein-2 were accreted together. After that, moderate heating of the CAI occurred. Grain boundaries of melilite of domein-2 were partially molten because of the high $\delta^{18}\text{O}$ compositions. The normally zoned melilite was overgrown on relicts of melilite during cooling.

Keywords: CAI, melilite, oxygen isotope, solid solution, chondrite

PPS021-05

Room:101

Time:May 23 09:30-09:45

Oxygen isotope zoning in reversely zoned melilite in Fluffy Type A CAI from Vigarano meteorite

Juri Katayama^{1*}, Shoichi Itoh¹, Hisayoshi Yurimoto¹

¹Natural History Sci., Hokudai

The oxygen isotopic variations of each mineral in the Ca-Al-rich inclusions (CAI) are due to mass-independent fractionation and plot along a CCAM line with slope of ~ 1 (Clayton et al., 1973). These variations indicate that CAI minerals were not derived entirely from a chemically homogeneous, well-mixed reservoir, but from mixing of ^{16}O -rich and ^{16}O -poor reservoir (e.g., Clayton., 1993). In previous in-situ oxygen isotope analyses, the oxygen isotope distribution of each CAI mineral go along a CCAM line results from the oxygen isotope exchange among ^{16}O -poor gas reservoirs and ^{16}O -rich CAI melt occurred by multiple partial melting process in the CAI forming region (Yurimoto et al., 1998). In addition, the oxygen isotopic compositions of each mineral in fine-grained CAI condensed from gas are enriched in ^{16}O (e.g., Krot et al., 2002). However, the relationship among two reservoirs in the CAI forming region is not clear.

Fluffy Type A CAI (FTA) condensed as solids from the hot solar nebular gas, based on their irregular shaped and the existence of reversely-zoned melilite crystals (MacPherson and Grossman, 1984). Therefore the intra-grain distribution of oxygen isotopes in FTA is critical to discussion of the oxygen isotopic composition of nebular gas, because these inclusions are believed to be direct condensates from the nebula (Yurimoto et al., 2008). In this study, we report the in-situ oxygen isotope distribution corresponding to the reversely-zoned melilite crystal in order to estimate the relationship between ^{16}O -rich and ^{16}O -poor gas reservoirs in the CAI forming region.

X-ray mapping with ~ 1 micron spatial resolution using FE-SEM-EDS determined compositional zoning of melilite crystals. Grain boundary was determined by orientation mapping using FE-SEM-EBSD. A line profile of oxygen isotope distribution of melilite crystal was obtained across the reversely zoning using Cameca ims-1270 SIMS with 3-5 micron spot.

Most melilite crystals in V2-01 FTA show the reversely zoned melilite using the estimation of grain boundary of melilite crystal with the effect of deformation and compaction in the parent body. The intra-grain distribution of oxygen isotopes in melilite crystals indicates that some melilite crystals show the oxygen isotope zoning with ~ 30 permil whereas shows no oxygen isotopic zoning. Two melilite single crystals (Grain 8 and 21) were estimated oxygen isotopic zoning with line profile correlated with reverse zoning. In the reverse zoning of Grain 8, ak content gradually change with the range of ~ 90 micron from core ($\sim \text{ak}_{14}$) to rim ($\sim \text{ak}_5$). The oxygen isotopic ratio changes with the range of ~ 40 micron from ^{16}O -poor ($\delta^{18}\text{O}_{\text{SMOW}} = -20$ permil, $\sim \text{ak}_8$) to ^{16}O -rich ($\delta^{18}\text{O}_{\text{SMOW}} = -30$ permil, $\sim \text{ak}_5$). In the reverse zoning of Grain 21, ak content gradually change with the range of ~ 65 micron from core ($\sim \text{ak}_{23}$) to rim ($\sim \text{ak}_2$). The oxygen isotopic ratio changes with the range of ~ 15 micron from ^{16}O -poor ($\delta^{18}\text{O}_{\text{SMOW}} = -15$ permil, $\sim \text{ak}_4$) to ^{16}O -rich ($\delta^{18}\text{O}_{\text{SMOW}} = -40$ permil, $\sim \text{ak}_2$). This means that the line profile shows, correlated with a gradual decrease in akermanite content, a change of oxygen isotopic ratios from ^{16}O -poor to ^{16}O -rich in the range of $15 \sim 40$ micron.

These results indicates that oxygen isotopic compositions of the gas reservoirs changed from ^{16}O -poor to ^{16}O -rich during crystallization of single melilite crystals. As results, there are gas reservoirs with oxygen isotope fluctuation changes from ^{16}O -poor to ^{16}O -rich in the CAI forming region.

A new constraint for chondrule formation: condition for rapid crystal growth along droplet surface

Hitoshi Miura^{1*}, Etsuro Yokoyama², Ken Nagashima³, Katsuo Tsukamoto¹

¹Tohoku University, ²Gakushuin University, ³Osaka University

Barred-olivine (BO) chondrules are characterized by parallel set(s) of olivine bar crystals, which are platy in three-dimension [1,2]. A BO chondrule usually has an olivine crystal that covers the chondrule surface (rim). The olivine rim has the same crystallographic orientation as the inner olivine platelets. Tsukamoto et al. succeeded to reproduce the rim structure from a forsterite melt droplet in their container-less crystallization experiment using aero-acoustic levitation technique [3]. They found that the droplet cooled very rapidly at a rate of $R_{cool} \sim 100 - 1000 \text{ K s}^{-1}$, and then crystallized within a very short period of time less than $\sim 1 \text{ s}$ at a large supercooling of $DT \sim 600 \text{ K}$. On the other hand, Tsuchiyama et al. also succeeded in reproducing the rim structure by evaporation in vacuum [4]. The cooling rate was $R_{cool} = 1000 \text{ K hr}^{-1}$, which is much slower than [3] by about three orders of magnitudes. Tsuchiyama et al. considered that the rim was formed by the rapid crystal growth along the droplet surface, which should become cooler than the interior by the latent heat of the evaporation. However, their hypothesis has not been verified yet.

To understand the formation mechanism of the rim structure, the crystal growth pattern inside the chondrule melt droplet should be investigated. We carried out numerical simulations of crystallization of a highly-supercooled melt droplet by using a phase-field method [5]. We considered the situation that a tiny crystal seeded at the droplet surface triggers crystallization of the droplet. We found that the rapid crystal growth along the droplet surface occurs when the cooling rate is considerably large. However, they did not investigate for a wide range of the supercooling of the droplet.

In this study, we investigated the condition of the rapid crystal growth along the droplet surface by using the phase-field method. We considered the cases that the seeding occurs when the surface of the droplet is supercooled by $DT_s = 200, 300, 400, 500, \text{ and } 600 \text{ K}$. The surface of the droplet cools at a constant heat flux; $q_s = 5 \times 10^8, 1 \times 10^9, 2 \times 10^9, 5 \times 10^9, \text{ and } 1 \times 10^{10} \text{ erg cm}^{-2} \text{ s}^{-1}$ for each DT_s . Because of the surface cooling, the droplet surface becomes cooler than the center by $dT_{c-s} \sim 30 - 600 \text{ K}$ for the droplet radius $r_d = 250 \text{ um}$ ($\text{um} = \text{micro-meter}$). We found that the rapid crystal growth along the droplet surface occurred when $dT_{c-s} \sim 100 - 200 \text{ K}$ or larger. The minimum value of dT_{c-s} for the rapid crystal growth along the droplet surface increases as DT_s increases. To derive the minimum value of dT_{c-s} analytically, we compared crystal growth timescales via two different routes inside the droplet; along the droplet surface, and across the droplet center. We found that the growth timescale along the surface becomes shorter than that across the center when $a = dT_{c-s} / DT_s > \sim 0.2$, which condition is rewritten by $R_{cool} > \sim 2000 (DT_s / 300 \text{ K}) (r_d / 250 \text{ um})^{-2} \text{ K s}^{-1}$. This condition is applicable for limited cases that satisfy the following two conditions; (a) crystal growth timescale is much shorter than a cooling timescale of the droplet, and (b) the supercooled droplet is a single component system, namely, the chemical composition of crystal is the same as the parent liquid. If the crystal growth kinetics depends on the growth direction, which usually comes from its crystal structure, we need small modification to the critical values of a and R_{cool} [5]. The new constraint for the rapid crystal growth along the droplet surface is applicable for limited cases, however, this is the first step to understand the formation mechanism of BO chondrule solidification texture.

Reference: [1] Tsuchiyama et al., *J. Geography*, **109**, 845-858, 2000 (in Japanese). [2] Noguchi, *Antarctic Meteorite Research*, **15**, 59-77, 2002. [3] Tsukamoto et al., *Antarct. Meteorites*, **24**, 179-181, 1999. [4] Tsuchiyama et al., *Geochim. Cosmochim. Acta*, **68**, 653-672, 2004. [5] Miura et al., *J. Appl. Phys.*, **108**, 114912, 2010.

Keywords: chondrule, barred olivine, formation condition, crystal growth

Japan Geoscience Union Meeting 2011

(May 22-27 2011 at Makuhari, Chiba, Japan)

©2011. Japan Geoscience Union. All Rights Reserved.



PPS021-07

Room:101

Time:May 23 10:00-10:15

Classification of micrometeorites bearing coarse-grained relict minerals

Naoya Imae^{1*}, Susan Taylor², Naoyoshi Iwata³

¹National Institute of Polar Research, ²U.S. ACRREL, ³Yamagata University

Micrometeorites bearing relict minerals survived the atmospheric entry heating have been studied.

Keywords: micrometeorites, classification, chondrites, meteorites

PPS021-08

Room:101

Time:May 23 10:45-11:00

REE pattern and oxygen isotopes in a unique granular-olivine inclusion from the Murchison (CM2) meteorite

Mutsuo Inoue^{1*}, Itoh Shoichi², Kimura Makoto³, Yurimoto Hisayoshi², Noboru Nakamura⁴

¹Kanazawa University, ²Hokkaido University, ³Ibaraki University, ⁴NASA Johnson Space Center

A homogeneous granular-olivine (Fa38.5) inclusion (MI-GO) carrying minor merrillite and nepheline was collected from the Murchison (CM2) meteorite, and analyzed for rare earth (REE; La, Ce, Nd, Sm, Eu, Gd, Dy, Er, Yb, and Lu) and other trace elements (K, Rb, Sr, and Ba) by isotope dilution, together with petrographical observation. The inclusion shows no evidence for aqueous alteration petrologically and chemically but indicates conspicuous REE fractionations; light-REE (L-REE) enriched, smoothly heavy-REE depleted pattern (La, $6.1 * CI$; CI-norm. La/Lu ratio = 3.0) with a large negative Eu anomaly (~70% negative), high FeO content (30%) and fractionated alkali abundances (CI-norm. K/Rb = 2.2). The observed bulk REE pattern is substantially different from those of aqueously altered CM chondrules and also from any kind of chondrules and CAIs from carbonaceous and unequilibrated ordinary chondrites (UOCs), but relatively similar to those of some kind of achondrite and of lunar KREEP basalts. The unique REE features, being similar to so-called geochemical fractionation, can not be explained as being due to nebular fractionation nor aqueous alteration processes, but are well understood as having been resulted from equilibrium partitioning of solid/melt and/or solid/solid interaction in the planetesimal setting. The holocrystalline texture, the occurrence of crystalline nepheline and homogeneous FeO-rich olivine suggest that MI-GO experienced melting and slow cooling or metamorphism and was then incooperated into the Murchison parent body during the early regolith-forming processes. To clarify the origin and precursor materials of MI-GO, we measured oxygen isotopic compositions in olivine groundmass using the Cameca ims-1270 ion microprobes. Combining the result of oxygen isotopic compositions, we discuss the formation process of MI-GO and the early planetary differentiation in the parent planetesimal.

PPS021-09

Room:101

Time:May 23 11:00-11:15

Diverse formation history recorded in two reduced-type carbonaceous chondrites RBT04143 and QUE97186

Hatsumi Ishida^{1*}, Tomoki Nakamura¹, Hitoshi Miura¹, Yuki Kakazu²

¹Tohoku University, ²Kyushu University

We have carried out mineralogical and oxygen isotopic analysis on two reduced-type carbonaceous chondrites, RBT04143, QUE97186, in order to estimate their formation and evolution processes.

According to polarized optical microscope observation, RBT04143 has porous matrix and rounded chondrules. On the other hand, the matrix of QUE97186 is highly compacted with porosity much lower than RBT04143 and chondrules are flattened to high aspect ratios and show a preferred orientation. This texture strongly suggests that the meteorite has experienced shock impact on the meteorite parent body. Olivine and pyroxene in QUE97186 chondrules show undulatory extinctions and planar deformation fractures. This result indicates that the meteorite experienced shock pressure around 20GPa based on the comparison to the results of previous shock recovery experiments (Nakamura et al., 2001) and polarizing microscope analysis (Stoffler et al., 1991).

To estimate the intensity of thermal metamorphism, we measured Fa# in fine-grained matrix olivine using FE-EPMA. As a result, Fa# in QUE97186 ranges from 40 to 60 but Fa# in RBT04143 shows a wider range (0 to 90). The wide Fa# variation in RBT04143 indicates that small silicate particles in the solar nebula have an extreme wide range of Fe/Mg ratios and RBT04143 has undergone least degrees of aqueous alteration and thermal metamorphism. Meanwhile, the narrow range of Fa# in QUE97186 is likely due to shock heating.

That the fine-grained matrix olivine escaped thermal metamorphism indicates CAI and chondrule in RBT04143 preserves the records of processes taken place in the early solar nebula. Oxygen isotope ratios of a type-B CAI and a type-II chondrule were measured by a secondary ion mass spectrometer (SIMS CAMECA ims-6f). The type-B CAI consists of melilite, fassaite, and diopside and these crystals locate from inner core to outer rim. The inner melilite shows ¹⁶O-poor composition, but outer diopside shows ¹⁶O-rich, suggesting that oxygen isotope exchange occurred between a nebula gas and the CAI at a temperature below melting point at which diffusion rates varies greatly between these minerals.

There are some relict Mg-rich olivine grains in the Type-II chondrule. Oxygen isotope ratios of Fe-rich olivine are homogeneous but the relict Mg-rich olivine is enriched in ¹⁶O. This indicates that the Mg-rich olivine preserves isotope composition of precursor grains, but other phases were melted and exchange oxygen with a nebula gas during heating.

Matrix in QUE97186 preserves evidence of impact. Some sulfides in the matrix are partially molten due to shock heating and the matrix was heated to temperature over 1170C. During cooling from this temperature, Fa# of fine-grained matrix olivine became homogenized. So as to estimate the cooling rate, simulation of changes of Fa# with time by considering size distribution of fine-grained olivine and Fe-Mg diffusion rates is in progress.

Keywords: CV3 carbonaceous chondrites

PPS021-10

Room:101

Time:May 23 11:15-11:30

Thermal metamorphism in type 3 Enstatite chondrites.

Mutsumi Komatsu^{1*}, Timothy Fagan¹, Takashi Mikouchi²

¹Earth Sciences, Waseda University, ²Earth and Planetary Sci., Univ. of Tokyo

Introduction:

Enstatite chondrites represent initial formation and metamorphism under highly reduced conditions. Like the other chondrite groups, the enstatite chondrites underwent various degrees of thermal metamorphism resulting in distinct petrologic types [1]. Type 3 chondrites are the least metamorphosed type among chondrite groups. For ordinary chondrites, Sears et al. [2] subdivided type 3 into ten finer divisions (type 3.0 through 3.9) using thermoluminescence (TL) sensitivity as an indicator of metamorphic grade. Subsequently, some mineralogical changes with increasing subtype have been identified [3]. An approach similar to that of [3] has been applied to enstatite chondrites [4]; however, a systematic understanding of metamorphic reactions has not been attained and metamorphic sub-types have not been established for enstatite chondrites. In this study, we examined 5 enstatite (EH3) chondrites in order to assess variations in texture and mineral compositions among the EH3 chondrites (ALHA81189, ALH84170, Sahara97096, Y-691, and PCA82518). We also compared these observations with EH4 (Indarch) and EH5 samples (St.Marks and LEW88180) to gain a broad perspective of metamorphism of EH chondrites.

Results and Discussion:

All of EH3 chondrites in this study are dominantly composed of FeO-poor pyroxene. Metallic and sulfide minerals occur as complex nodules which are composed of combinations of troilite, Fe-Ni metal, perryite, niningerite, djerfisherite, and daubreelite. Occasionally, oldhamite is also present.

ALHA81189 contains well-defined chondrules and chondrule fragments. Many chondrules are rimmed by silica or silica-rich rims in ALHA81189 and Y-691, whereas silica or silica-rich rims are not as abundant in ALH84170 and Sahara97096. In PCA82518, silica-rich rims were not identified. Instead, euhedral silica is observed inside chondrules.

Sulfide nodules are abundant in all EH3s. Sulfide/metal nodules in ALHA81189, ALH 84170 and Y-691 have sizes and shapes similar to silicate chondrules and are composed of combinations of troilite, kamacite, daubreelite, and niningerite. Generally, troilite and daubreelite occupy the cores of the spherules whereas kamacite usually occurs in the outer portions. Sulfides are more dispersed in PCA82518; the core-rim structure as described above is absent. In contrast, mixed sulfide/metal nodules are rare and sulfides tend to occur as dispersed crystals in Indarch (EH4), St. Marks (EH5) and LEW 88180 (EH5).

The Fa content of olivine, Fs content of pyroxene, and Ti and Cr contents in troilite show wide ranges of composition in the EH3 chondrites. Ti concentrations of troilite in ALHA81189 are lower than in the other EH3s, and those in PCA are the highest.

Based on the textural characteristics of EH3 chondrites, we can subdivide EH3s into 3 distinct groups: (1) Primitive, ALHA81189 and Y-691; (2) low degree of metamorphism, ALH84170 and Sahara 97096; moderately metamorphosed, PCA82518. This trend is supported by the chemical compositions of pyroxene and troilite; primitive EH3s have high Fs content in pyroxene and low Ti content in troilite, whereas metamorphosed EH3s have lower Fs content in pyroxene and higher Ti content in troilite. These results suggest that the reduction (lower $f(O_2)$) occurred during thermal metamorphism [5].

References: [1] Zhang et al. (1995) JGR, 100, E5, 9417-9438. [2] Sears et al. (1983) LPS XIV, 682-683. [3] Grossman J. N. and Brearley A. J. (2005) Meteoritics & Planet. Sci., 40, 87-122. [4] Bendersky et al. (2007) LPS, XXXVIII, 2077. [5] Fagan T. J. et al. (2010) LPS XXVII, 1534.

Keywords: meteorites, chondrites, metamorphism

PPS021-11

Room:101

Time:May 23 11:30-11:45

Mn-Cr dating of dolomite in the Ivuna CI chondrite

Wataru Fujiya^{1*}, Naoji Sugiura¹, Yuji Sano¹

¹The Univ. of Tokyo

CI chondrites are compositionally the most primitive rocks among the solar system materials, although they experienced pervasive aqueous alteration. In order to decipher their geological history, it is important to determine the timescale of the aqueous activity in the CI chondrite parent body.

⁵³Mn-⁵³Cr systematics (⁵³Mn decays to ⁵³Cr with a half-life of 3.7 Myr) of dolomite and breunnerite measured with ion probes have been reported for the Orgueil CI chondrite (e.g. Hoppe et al., 2007). For the Ivuna CI chondrite, there is only one report on dolomite. Hence, further investigations are needed for the accurate Mn-Cr age determinations. Here we report Mn-Cr systematics of six dolomite grains in Ivuna.

Six dolomite grains in Ivuna were analyzed for Mn-Cr systematics with the NanoSIMS installed at Atmosphere and Ocean Research Institute, the Univ. of Tokyo. Their Mn concentrations range from 0.7 to 2.7 wt.%. ⁵³Ca⁺, ^{52,53}Cr⁺ and ⁵⁵Mn⁺ were measured with the O⁻ primary ion beam (~5 micrometers in diameter, ~1 nA). The ⁵⁵Mn/⁵²Cr relative sensitivity factor (RSF) of 0.690 is determined using a synthetic calcite standard doped with Mn and Cr (Sugiura et al., 2010). Errors on ⁵³Cr/⁵²Cr and ⁵⁵Mn/⁵²Cr ratios are based on the counting errors. ⁵³Cr excesses of the Ivuna dolomite are represented as permil deviations from the ⁵³Cr/⁵²Cr ratio of the standard assumed to be 0.1134 (Lodders et al., 2009).

Obtained ⁵³Cr excesses are well correlated with ⁵⁵Mn/⁵²Cr, which indicates the in-situ decay of ⁵³Mn. All data lie on a single regression line in the isochron diagram (i.e., no difference is found among slopes of the six grains) and the slope of the best fit line for the whole data corresponds to (⁵³Mn/⁵⁵Mn)₀ of (2.64 +/- 0.44) x 10⁻⁶. Then an absolute age of 4562.5 +/- 0.8/-1.0 Ma is calculated for dolomite in Ivuna using the LEW86010 angrite as a time anchor (Amelin, 2008; Lugmair and Shukolyukov, 1998).

The present data for dolomite in Ivuna gives a younger age than that in Orgueil reported by Hoppe et al. (2007) and Petit et al. (2009). However, these studies used silicate standards for calibration of ⁵⁵Mn/⁵²Cr ratios of dolomite, which resulted in systematic errors in the obtained ages. If the RSFs are corrected, then the Mn-Cr ages of the Orgueil dolomite become consistent with that of the Ivuna dolomite. The Ivuna dolomite in this study is older than the Orgueil and Ivuna dolomite reported by Endress et al. (1996), which is unlikely due to the difference in the RSFs used. The reason for this discrepancy is unknown at this time.

Fujiya et al. (2011) reported Mn-Cr ages of calcite and dolomite in four CM chondrites, indicating that calcite and dolomite in CM and CI chondrites formed around the same time. Because calcite precipitation appears to have preceded dolomite formation (de Leuw et al., 2010), our data imply contemporaneous accretions of the CI and CM chondrite parent bodies and dolomitization occurred soon after calcite precipitation.

On the other hand, it seems that individual breunnerite grains in Orgueil show variable and younger ages than those of dolomite grains (Hoppe et al. 2007; Petit et al., 2009). Therefore, we conclude that the breunnerite formation persisted for at least 7 Myr following dolomite formation. Given that the Mn-Cr ages in Petit et al. are biased due to the RSFs, breunnerite formation (and therefore, aqueous alteration) in Orgueil lasted until ~4553 Myr (at least 10 Myr after dolomite formation in Ivuna).

Keywords: dolomite, CI chondrite, Mn-Cr dating, aqueous alteration

PPS021-12

Room:101

Time:May 23 11:45-12:00

Oxygen isotopic compositions of silicate grains associated with D-rich carbonaceous matters in a carbonaceous chondrite

Minako Hashiguchi^{1*}, Sachio Kobayashi², Hisayoshi Yurimoto¹

¹Natural History Sci., Hokkaido Univ., ²CRIS, Hokkaido Univ.

Organic matters enriched in D and/or ¹⁵N in chondrites are believed to have formed in cold molecular cloud and/or outer protoplanetary disk. The organic matters would be produced in ice coatings on interstellar dust grains in the cold interstellar cloud [e.g. 1].

In our previous study, we discovered D-rich carbonaceous matters in NWA 801 (CR2) carbonaceous chondrite using hydrogen isotope imaging, and classified their morphology [2]. Hydrogen isotopic compositions of these carbonaceous matters are 1360-11000 permil of delta-D. Some D-rich carbonaceous matters in the NWA 801 are ring shaped globules containing a silicate grain in the center (ring globule), and aggregates with silicate grains (globule aggregate).

In this study, we focus on the silicate grains associated with D-rich carbonaceous matters. Their oxygen isotope compositions were measured by isotope imaging using isotope microscope in Hokkaido University [3].

Oxygen isotopic compositions of the silicate grains analyzed here are not different from the isotopic composition of solar system. The results suggest that these silicate grains have formed in the solar system. Therefore, it is plausible that the ring globules and the globule aggregates were formed on the silicate grains in outer protoplanetary disk in the early solar system. However, it is difficult to reject a possibility that most presolar grains in the cold molecular cloud have similar oxygen isotopic compositions with materials formed in the solar system and the ring globules and globule aggregates have formed in the cold molecular cloud.

In the future work, we will measure the oxygen isotopic compositions of more numbers of ring globules or globule aggregates. The dataset will be helpful to reveal formation region of D-rich carbonaceous matters in meteorites.

References

- [1] Li, A. and Greenberg, J. M. (1997) *Astron. Astrophys.*, 323, 566
- [2] Hashiguchi, M. et al. (2010) 73rd Annual Meeting of the Meteoritical Society., 5181
- [3] Yurimoto, H. et al. (2003) *Appl. Surf. Sci.*, 203, 793

Keywords: Carbonaceous chondrite, Organic material, Oxygen isotopic composition, Isotopography

PPS021-13

Room:101

Time:May 23 12:00-12:15

New insight into origin and evolution of insoluble organic matter in meteorites

Yoko Kebukawa^{1*}, Ying Wang¹, George Cody¹

¹Carnegie Institution of Washington

Organic matter in meteorites provides us clues to understand the early Solar System history. Our recent study revealed that insoluble organic matter (IOM) in primitive chondritic meteorites is predominantly derived from the polymerization of interstellar formaldehyde with incorporation of ammonia, evidenced by molecular spectroscopic characters. Here we show molecular structures of laboratory synthesized formaldehyde polymer and compare with the formose solids to chondritic IOM using various spectroscopic methods; solid state ¹³C nuclear magnetic resonance (NMR), Fourier transform infrared (FTIR) spectroscopy and X-ray absorption near edge structure (XANES). We will discuss about the kinetics of polymer yield, and effects of silicate minerals coexisting with chondritic organic matter. Isotopic exchange experiments with formaldehyde polymer and water also can explain the origin of deuterium enrichment in the IOM from carbonaceous chondrites. We featured ¹H-²H cross polarization NMR which allows us to see site-specific deuterium enrichment in organic polymers. The results show that organic hydrogen is very exchangeable with water. The deuterium enrichment of chondritic IOM could be explained by the deuterium exchange with water during aqueous alteration.

The final molecular structure of chondritic IOM has been shown to reflect the extent of parent body processing, and to have significant variations among chondrite classes and groups. The principal inference has been that the molecular structure of IOM changes as a result of environmental conditions in the parent body. Our recent studies of individual lithology of the Tagish Lake meteorite provides insight into the wide range of molecular structure complexity that existed locally in a single parent body. We conducted heating experiments of most pristine IOM from Tagish Lake. The molecular structure evolution observed in Tagish Lake is representable with flash heating with several hundred degree C. Thus, the changes in Tagish Lake IOM from different lithologies may reflect differing degrees of flash heating due to impact processes.

Keywords: insoluble organic matter, chondrites, NMR, FTIR, XANES

PPS021-14

Room:101

Time:May 23 12:15-12:30

Three-dimensional observation of organic nanoglobules by microtomography and evaluation of CT images by image simulation

Tooru Matsumoto^{1*}, Akira Tsuchiyama¹, Keiko Nakamura-Messenger², Michael.E.Zolensky², Tsukasa Nakano³, Kentaro Uesugi⁴

¹Earth and Space Sci., Osaka Univ, ²NASA Johnson Space Center, ³GSJ/AIST, ⁴JASRI

Spherical organic matters called organic nanoglobules of a few hundred micrometers in typical size were found in carbonaceous chondrites, IDPs, and dust from comet 81P/Wild2 [1-3]. Most of them have hollow structures. It has been suggested that the organic nanoglobules were formed from organics-ice particles in the molecular cloud or the protoplanetary disk in the solar system [4]. Aqueous alteration of organic matters is also suggested as alternative possible formation processes [1]. If one of the hypotheses is true, hollow regions of the globules might be filled with H₂O-rich ices or fluids. However they have not been detected because they had been lost during destructive observations, such as transmission electron microscope (TEM) observation, in the previous studies.

In the present study, we tried to observe organic globules non-destructively using synchrotron radiation-based absorption-contrast imaging X-ray microtomography [5] in order to determine the existence of fluids in the hollows of nanoglobules. The imaging experiments were made at the beamline BL47XU of SPring8 with the photon energy of 7.0 keV. CT images were reconstructed from 1800 projections and successional CT images of about 800 slices were obtained for the 3-D structure of Tagish Lake meteorite. The voxel size in the CT images is 40.8 nm³. Then, we microtomed some samples and observed ultra-thin sections under a TEM. Comparison between the CT and the TEM images showed that nanoglobules can be observed in the CT images. But CT images of nanoglobules are affected by X-ray refraction. So we could not determine materials in nanoglobules from CT images alone. There are many spherical objects as candidates of organic nanoglobules in the CT images.

In order to identify nanoglobules and to determine whether or not any fluids are present in the hollows, we tried to evaluate CT images by simulating CT images by considering X-ray absorption and refraction for nanoglobules with hollow or water, which are surrounded by saponite, a main constituent mineral of Tagish Lake meteorite matrixes. We calculated transmittance of X-rays that pass the sample with absorption and refraction and reach a detector. Actual tomography experiments were performed under an imaging system with a Fresnel zone plate (FZP). The location of the detector in the simulation corresponds to a focal spot of the FZP. Simulated CT images were made by reconstruction with the pixel sizes of the detector (40.8 nm) and measured point spread function (FWHM = 360 nm). Simulated CT images indicated that nanoglobules containing water cannot be distinguished from those without hollow in CT images. When organic rims are thin, CT images of nanoglobules with hollow cannot not be distinguished from those of simple spherical pores. The effective spatial resolution of nanoglobules is about 300 nm. Comparison between CT images of nanoglobules identified by the TEM observation and simulated CT images suggested that this nanoglobules might not contain any water.

The simulation also revealed that three-dimensional shape of nanoglobule can be estimated by CT images. Three-dimensional distribution of nanoglobules can be also obtained by CT images. We can grind the sample to the position right above a nanoglobule detected by tomography and analyze a fluid in the nanoglobule using a microanalysis, such as nano SIMS, if fluid is reserved.

[1] Nakamura K. et al (2002) *Int. J. Astrobiol.*, 1, 179. [2] Messenger S. et al. (2008) *LPS XXXIX*, Abstract #2391. [3] De Gregorio B. T. (2009) *LPS XXXX*, Abstract #1130. [4] Nakamura-Messenger K. et al (2006) *Science*, 314 1439-1442. [5] Uesugi K et al (2006) *Proceedings of SPIE6318:63181F*.

Keywords: X-ray microtomography, organic nanoglobule, carbonaceous chondrite, image simulation